Experimental and CFD analysis of flow through venturimeter to determine the coefficient of discharge

Nikhil Tamhankar
Department of Mechanical Engineering
Smt. Kashibai Navale College of Engineering, Pune, Maharashtra, India

Amar Pandhare
Department of Mechanical Engineering
Smt. Kashibai Navale College of Engineering, Pune, Maharashtra, India

Ashwinkumar Joglekar
Department of Mechanical Engineering
Smt. Kashibai Navale College of Engineering, Pune, Maharashtra, India

Vaibhav Bansode
Department of Mechanical Engineering
Smt. Kashibai Navale College of Engineering, Pune, Maharashtra, India

Abstract- The pressure distribution along the walls of venturi tube is widely used in many industry tests and applications. The authors have made an attempt to study and prepare a computational model of a venturimeter, which can be used as an efficient and easy means for calibration of the instrument instead of costly experimental methods. The research covers the following aspects: to study the theory of the venturimeter and calculate the data theoretically by using Bernoulli's equation, to analyse the experimental data and to plot graphs for it. The focus here is to analyse the pressure variations across the venturi section by means of Ansys Fluent 13.0, a commercial CFD code, which explores the use of computational methods to compute the flow parameters in the tube. The study aims at comparing the results calculated by both, the computational and experimental methods. An effort is made to check the validity of Bernoulli's equation when applied to the steady flow of water in a tapered duct and to calibrate the venturi as a flowmeter by calculating the coefficient of discharge.

Keywords – venturimeter, computational, calibration, coefficient of discharge

I. INTRODUCTION

The venturi meter is an obstruction meter named in honor of Giovanni Venturi (1746–1822), an Italian physicist who first tested conical expansions and contractions. The original, or classical, venturi was invented by a U.S. engineer, Clemens Herschel, in 1898. It consisted of a 21° conical contraction, a straight throat of diameter *d* and length *d*, then a 7 to 15° conical expansion. The discharge coefficient is near unity, and the non recoverable loss is very small. The modern venturi nozzle consists of an ISA 1932 nozzle entrance and a conical expansion of half-angle no greater than 15°. It is intended to be operated in a narrow Reynolds-number range of 1.5×10^5 to 2×10^6 [3]. Venturi meters consist of a short length of pipe shaped like a vena contracta, or the portion with the least cross-sectional area, which fits into a normal pipe-line. The obstruction caused to the flow of liquid at the throat of the venturi produces a local pressure drop in the region that is proportional to the rate of discharge. This phenomenon, using Bernoulli's equation, is used to calculate the rate of flow of the fluid flowing through the pipe. Nowadays, it is necessary to perform the calibration tests of the flow meters in order to find out the accuracy of the instrument. These can be done by calculating the discharge coefficient of the venturi. Although experimental procedures offer a good result, they are often time consuming. Hence a more sophisticated method of testing the flow meter is through numerical methods. Due to a variety of commercial CFD codes being available in the market, it is possible to obtain

more accurate results which take less time. These results can then be compared with the initial experimental results to calibrate the instruments.

II. MODEL GEOMETRY AND MESH GENERATION

The domain selected for the analysis was the venturi section. On both sides of the venturi section a length of approximately five times the diameter of the pipe was taken into consideration as part of domain in order to get fully developed turbulent flow. The 3D geometry of the domain was prepared in CATIA V5 R18 and the mesh was generated in Hypermesh. The mesh interior is made of 114452 tetrahedral cells. There are 237917 triangular faces and the number of nodes is 23979. The maximum aspect ratio is 15.6339.

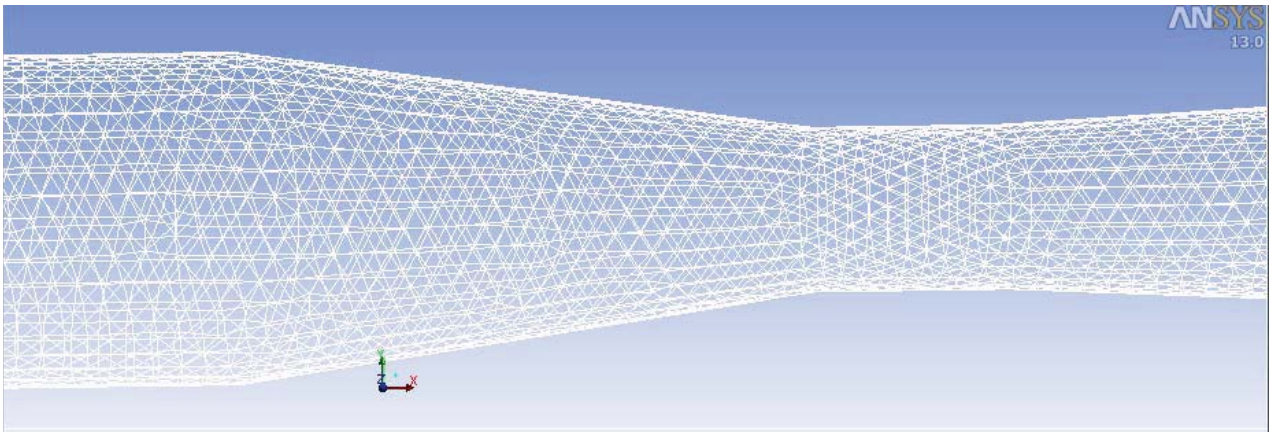

Figure 1. Mesh

III. CFD ANALYSIS OF THE FLOW

Basically, CFD is the numerical solution of governing equations of motion, which describe the flow behavior of fluids. In the modeling, mass, momentum, energy conservation equations (if necessary) must be satisfied. The governing equations for steady incompressible flows are:

$$\rho\, \partial/\partial x\, (u\_i\ ) = S\_(m.) \qquad (1)$$

The mass conservation equation is valid for both incompressible and compressible flows. The source term S_m is the mass added to the continuous phase from the dispersed phase. The momentum conservation equation for steady flow is written as,

$$\partial/(\partial x\_j\ )\ [\rho u\_i\, u\_j\ ] = (\partial P\_i)/(\partial x\_i\ ) + (\partial \tau\_ij)/(\partial x\_j\ ) + \rho g\_i + F\_i \qquad (2)$$

Where Pi is the static pressure, ρg_i is the gravitational body force and F_i is the external body force [5].
The Realizable k-ε turbulence model with enhanced wall treatment was selected to model the flow which is superior to the Standard k-ε model for the prediction of separated flows. The solution was computed in the commercial CFD code Fluent 13.0, in which the pressure based solver, was selected for this particular case. The heat transfer from the wall of the domain was neglected. The velocity inlet boundary condition was used to define the volume flow rate at the flow inlet and the outflow boundary condition at the outlet was set to 1. The hydraulic diameter and turbulent intensity at the inlet were specified as 0.026m and 5% respectively. The adiabatic wall condition was used at the wall region. The governing equations were solved using a segregated solver in which the momentum equations are solved first, and then the continuity equation and finally the pressure and velocity are updated. The SIMPLE algorithm (Patankar and Spalding) was used for coupling between the velocity and pressure fields. The numbers of iterations specified were 200. The pressure drop across the convergent portion of the venturi was calculated using the code and these values were used to calculate the discharge coefficient using the simple Bernoulli's equation. The discharge coefficient was calculated for three different values of flow rates.

Table -1 Input parameters and boundary conditions

Type of solver	**Pressure based solver**
Energy model	**Off**
Material	**Water**
Density of water	**996 kg/ m ^{3}**
Turbulent intensity	**5%**
Hydraulic diameter	**0.026m**
Area of measuring tank	**0.1353 m ^{2}**
Solution method	**SIMPLE scheme**
Solution initialization	**From inlet**
Number of iterations specified	**200**

IV. EXPERIMENTAL TESTS

The flow calibration facility is set-up for the calibration of differential pressure type of flow elements by accurately measuring the weight of water passing through the flow element and collected in collection tank over a given time. The water is stored in a sump tank and pumped through supply line to maintain constant head and desired flow. The calibration setup has a venturimeter and an orifice meter. The orifice meter valve is closed completely and for the venturimeter, the desired flow in supply and calibration line is achieved by control valves in supply line, calibration line and pump bypass line [4]. Readings taken are time taken for 100 mm rise in water level in the measuring tank and the manometric head indicated by the differential manometer. Readings are taken for three different values of flow rates. The observations H1 and H2 indicate the manometric deflections on both sides of the scale.

Table -2 Setup parameters

Sump tank	**1210 x 410 x 410 mm^3**
Measuring Tank	**410 x 330 x 410 mm^3**
Diameter of venturi throat	**13 mm**
Area of venturi throat (rpm)	**1.32 x 10 $^{-3}$ m ^{2}**
Diameter of convergent cone	**26 mm**
Area of convergent cone	**6.3 x 10 $^{-4}$ m ^{2}.**
Area of measuring tank	**0.1353 m ^{2}**
Manomter	**Differential U-tube type**

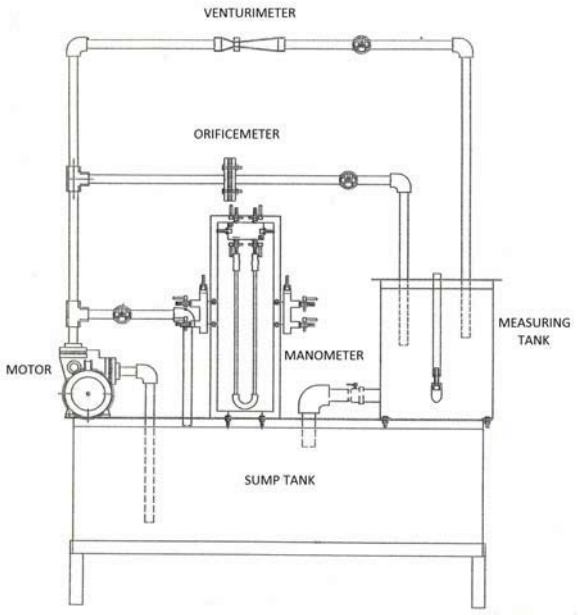

Figure 2. Experimental setup

Table -3 Observation readings

Reading No.	H1(cm)	H2(cm)	Time required for 100 mm rise of water (sec)
1	1	1.5	51
2	3	2.5	27
3	3.9	3.5	21.8

V. RESULTS AND DISCUSSIONS

The results discussed are the volume flow rates, the discharge coefficients and the various plots for pressure distribution, velocity vectors, turbulent kinetic energy and graphs for the same.

A. Volume flow rates:

The Q_{Actual} for CFD analysis was calculated as:

$$Q_{Actual} = (\text{Cross section area at throat}) \times (\text{Velocity at throat}) \quad (3)$$

The $Q_{Theoretical}$ was calculated by calculated the pressure drop between the start of the convergent cone and the mid section of the throat. These values were calculated by constructing two cross section planes at these two regions using the CFD code and then taking the difference of the values of average absolute pressures at these sections. This pressure difference was converted in meters of water and substituted in the formula for calculating theoretical discharge in a venturi.

$$Q_{Theoretical} = K \sqrt{2gH} \quad (4)$$

Where *H* is pressure drop expressed in meters of water column and K is the coefficient of venturimeter given by

$$K = (A1 \times A2)/ \sqrt{((A1)^2-(A2)^2)} \quad (5)$$

The actual volume flow rate for experimental analysis were calculated by measuring time taken for 100 mm rise in measuring tank while theoretical flow rate was calculated by measuring the pressure drop indicated by the manometer between the two sections.

B. Coefficient of discharge:

The coefficient of discharge obtained from both, the experimental tests and the CFD analysis are as follows**:**

Table -4 Results

Reading No.	Experiment	CFD analysis
1	0.9724	0.9619
2	0.9592	0.9689
3	0.9779	0.9692

As we can see from Table 4, the results obtained are within 5% accuracy.

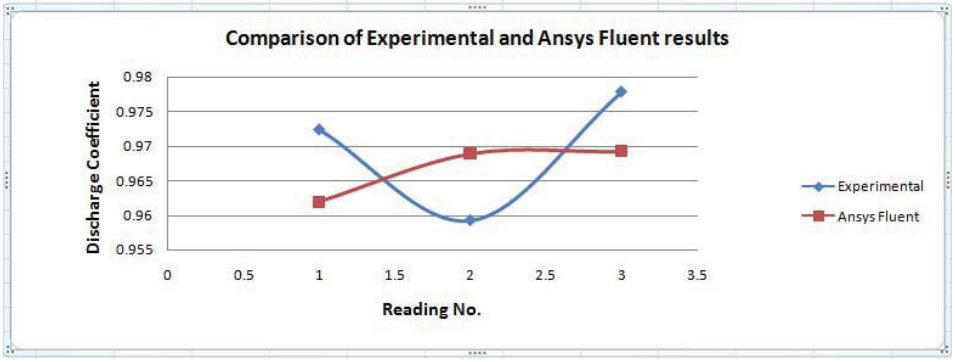

Figure 3. Comparison of experimental and Ansys Fluent results

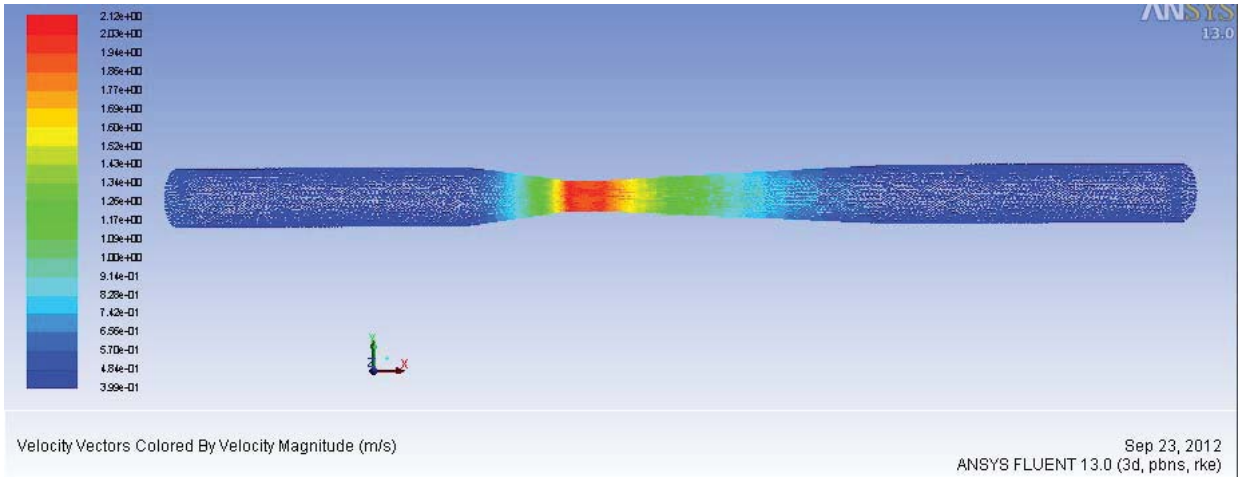

Figure 4. X velocity vectors

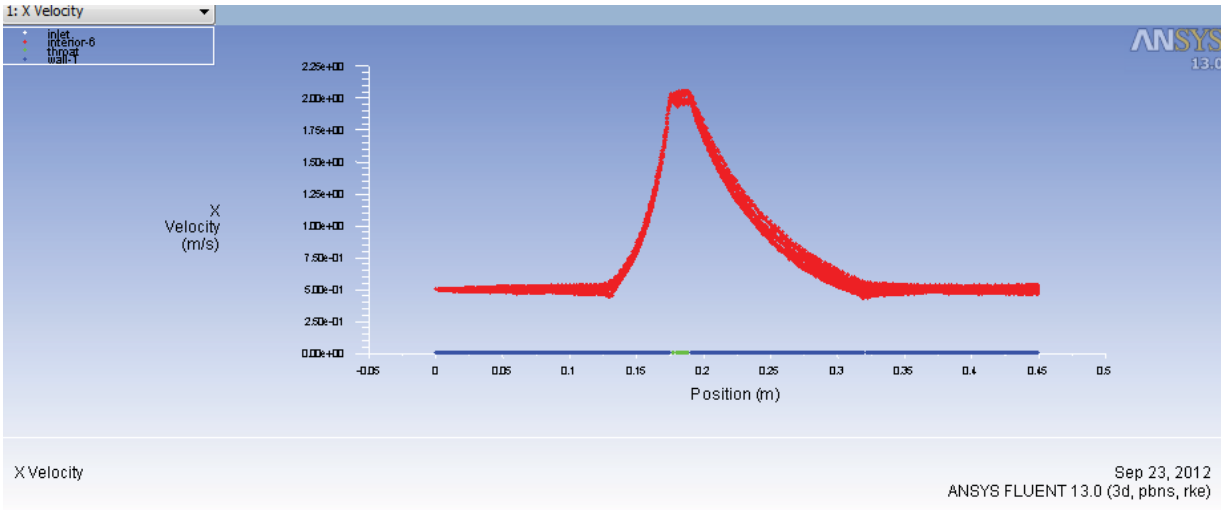

Figure 5. X velocity versus position

Figure 4 and Figure 5 show the variation of velocity in the X direction as well as the velocity vectors. It is evident that the maximum value of velocity occurs at the throat of the venturi. Also the variation of velocity in the divergent section of the venturi is gradual as compared to the convergent section.

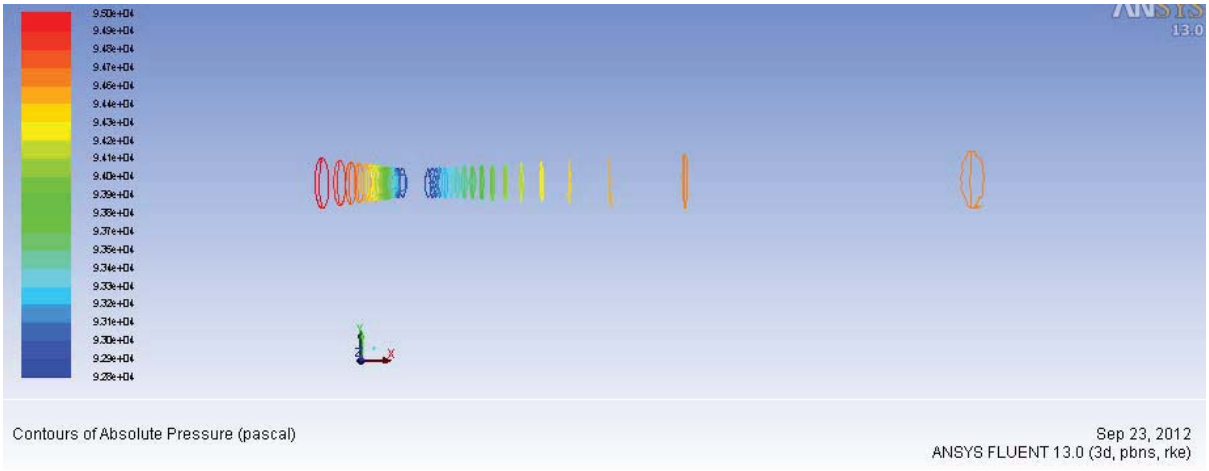

Figure 6. Contours of absolute pressure

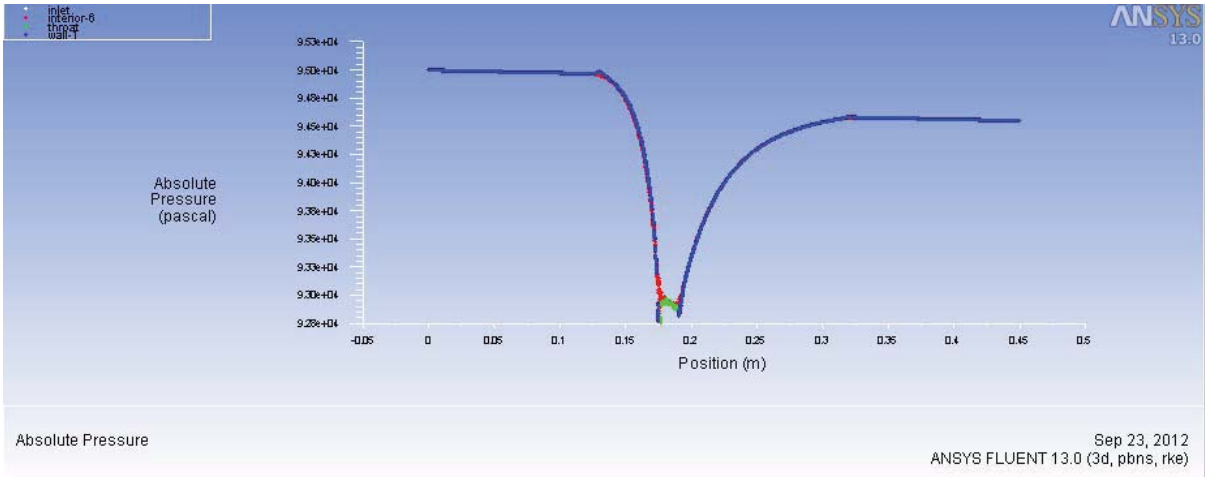

Figure 7. Absolute pressure versus position

Figure 6 and Figure 7 show the contours and the variation of absolute pressure in the X direction. As we can see, the pressure goes on reducing in convergent section and attains minimum value at the throat. From the graph, it is evident that the pressure regained after the divergent section is not equal to the initial pressure in the pipe. This shows that frictional losses occurring in the venturi section reduce the pressure of the flow.

VI. CONCLUSIONS

A brief summary and various conclusions drawn from the observations and calculations are as follows

- The values of discharge coefficient obtained from experimental tests and CFD simulation are very close to each other.
- The accuracy of results is within 5%.
- The results do not match each other exactly due certain assumptions made the CFD analysis.
- Calibration of the venturimeter was successfully carried out.
- Various plots and graphs for velocity and internal pressure distributions were analyzed.
- It can be inferred that such computational models can provide an efficient and accurate method for re-calibrating flowmeters instead of employing costly and time consuming experimental methods.

REFERENCES

[1] Anderson, J. D. (1995). Computational fluid dynamics: The basics with applications (6th Ed.). New York, NY: Mcgraw Hill, Inc.

[2] Versteeg, H.K. & Malalasekera, W. (2007). *An Introduction to Computational fluid dynamics: The Finite Volume Method* (2nd Ed), New Jersey: Pearson education ltd

[3] Cengel, Y. A. & Cimbala J. M. (2010). *Fluid Mechanics: Fundamentals and applications* (2nd Ed), Noida, UP, India: Tata McGraw-Hill Education.

[4] Sapra, M.K., Bajaj, M., Kundu, S.N., Sharma, B.S.V.G. (2011). *Experimental and CFD investigation of 100 mm size cone flow elements*. Flow Measurement and Instrumentation, 22, 469–474.

[5] Singh, R.K., Singh, S.N., Seshadri, V. (2009). *Study on the effect of vertex angle and upstream swirl on the performance characteristics of cone flowmeter using CFD*. Flow Measurement and Instrumentation, 20, 69–74.

[6] Hojat Ghassemi, Hamidreza Farshi Fasih (2011). *Application of small size cavitating venturi as flow controller and flow meter*. Flow Measurement and Instrumentation, 22, 406–412.

[7] Denghui He, Bofeng Bai (2012). *Numerical investigation of wet gas flow in Venturi meter*. Flow Measurement and Instrumentation, 28, 1–6.

[8] Singh, Rajesh Kumar, Singh, S.N., Seshadri V. (2010). *CFD prediction of the effects of the upstream elbow fittings on the performance of cone flowmeters*. Flow Measurement and Instrumentation, 21, 88–97.

[9] Reader-Harris, M.J., Brunton, W.C., Gibson, J.J., Hodges, D., Nicholson, I.G. (2001). *Discharge coefficients of Venturi tubes with standard and non-standard convergent angles*. Flow Measurement and Instrumentation, 12, 135–145.